

1 Supplementary Information for

2

3 Widespread submarine volcanic eruptions and tectonics revealed in the

4 northwest Pacific Ocean

5

6 Juan Zhu¹, Lianxing Wen^{2*}

7

⁸ ¹Laboratory of Seismology and Physics of Earth's Interior, School of Earth and Space
⁹ Sciences, University of Science and Technology of China; Hefei, 230026, China.

10 ²Department of Geosciences, State University of New York at Stony Brook; NY 11794, USA.

11

12 *Correspondence to: Lianxing.Wen@stonybrook.edu (L.W.)

13

14 Table of Contents

15 Supplementary Note 1 | Hydroacoustic data.

16 Supplementary Note 2 | Elimination of air-gun shot sources and other disturbed sources.

17 Supplementary Note 3 | Verification of explosive submarine volcanic eruption.

18 Supplementary Fig. 1 | H11 hydrophone array used to study explosive submarine volcanoes.

19 Supplementary Fig. 2 | Detection discriminants for an explosive submarine volcanic eruption

20 at hydrophone station H11S2.

21 Supplementary Fig. 3 | Detection discriminants for an explosive submarine volcanic eruption

22 at hydrophone station H11S3.

23 Supplementary Fig. 4 | Waveform characteristics of air-gun shot signals.

24 Supplementary Fig. 5 | Similar seismic discriminants for an example air-gun shot indicated in

25 Supplementary Fig. 4 and an explosive submarine volcanic eruption.

26 Supplementary Fig. 6 | Source characteristics of air-gun shot signals.

27 Supplementary Fig. 7 | Discolored water spreading in a lotus pattern at 04:51 UTC on February

28 4, 2010 observed by a local flyover photo near the sea surface of the Fukutoku-Okanoba.

29 Supplementary Fig. 8 | Detection and verification of explosive submarine volcanic eruptions

30 of Fukutoku-Okanoba in the northwest Pacific Ocean.

31 Supplementary Fig. 9 | Detection and verification of explosive submarine volcanic eruptions

32 of Kaitoku in the northwest Pacific Ocean.

33 Supplementary Fig. 10 | Detection and verification of explosive submarine volcanic eruptions

34 of Ahyi in the northwest Pacific Ocean.

35 Supplementary Fig. 11 | Detection and verification of explosive submarine volcanic eruptions

36 of South Sarigon in the northwest Pacific Ocean.

37 Supplementary References

38 **Supplementary Note 1 | Hydroacoustic data**

39 We use continuous hydroacoustic data recorded from 1 January, 2010 to 13 December, 2022
40 by the H11 hydrophone array located near the Wake Island of the Northwest Pacific Ocean
41 (Supplementary Fig. 1). The H11 hydrophone array is operated by the CTBTO and consists of
42 two hydrophone subarrays (H11N and H11S) separated by about 135 km. Each subarray is
43 equipped with three hydrophone stations situated in a triangle of a 2.0-km spacing
44 (Supplementary Fig. 1). Hydrophones are moored in the SOFAR channel axis at water depths
45 of 731 m (H11N1), 732 m (H11N2), 729 m (H11N3), 750 m (H11S1), 742 m (H11S2) and 726
46 m (H11S3) (Supplementary Fig. 1). Hydrophone sensors have a flat frequency response from
47 10 Hz to 100 Hz and a sampling rate of 250 Hz¹. Data are band-pass filtered between 6 Hz and
48 60 Hz in accordance with the frequency character of the signals typically associated with
49 submarine volcanic activity²⁻⁵ while minimizing potential noise contamination in other
50 frequencies from ocean microseism⁶, marine mammal vocalization⁷, and commercial
51 shipping⁸.

52

53 **Supplementary Note 2 | Elimination of air-gun shot sources and other disturbed sources**

54 Air-gun shot sources are underwater anthropogenic explosive sources in the shallow water that
55 could last for tens of hours with usually a fixed time interval between consecutive signals
56 (Supplementary Fig. 4)^{9,10}. They satisfy the discriminant criteria for an explosive submarine
57 volcanic eruption, with a short and impulsive waveform, and inverted dispersion of frequency,
58 and an irregular slow-decaying spectrum of the recorded signals (Supplementary Fig. 5).
59 Typically, air-gun shot signals exhibit highly similar spectrum and waveforms (Supplementary
60 Fig. 6). We remove the air-gun shot sources based on regularity of the time intervals and
61 similarity of the waveforms between consecutive signals. In the first step, we identify air-gun

62 shot signals based on the equal time intervals between consecutive signals. If the two time-
63 intervals range in 8-40 s and are equal or multiplicative between consecutive signals in each
64 three subsequent signals, we identify the detected events as air-gun shots and remove them
65 from the detection list. In the second step, we randomly select an identified air-gun shot event
66 as a template and remove the events that have waveform cross-correlation coefficients larger
67 than 0.6 with the template. The templates are selected within each 3-hour from those air-gun
68 shots identified in the first step with a signal amplitude greater than 0.8 times the largest
69 amplitude of all the identified events in the time period.

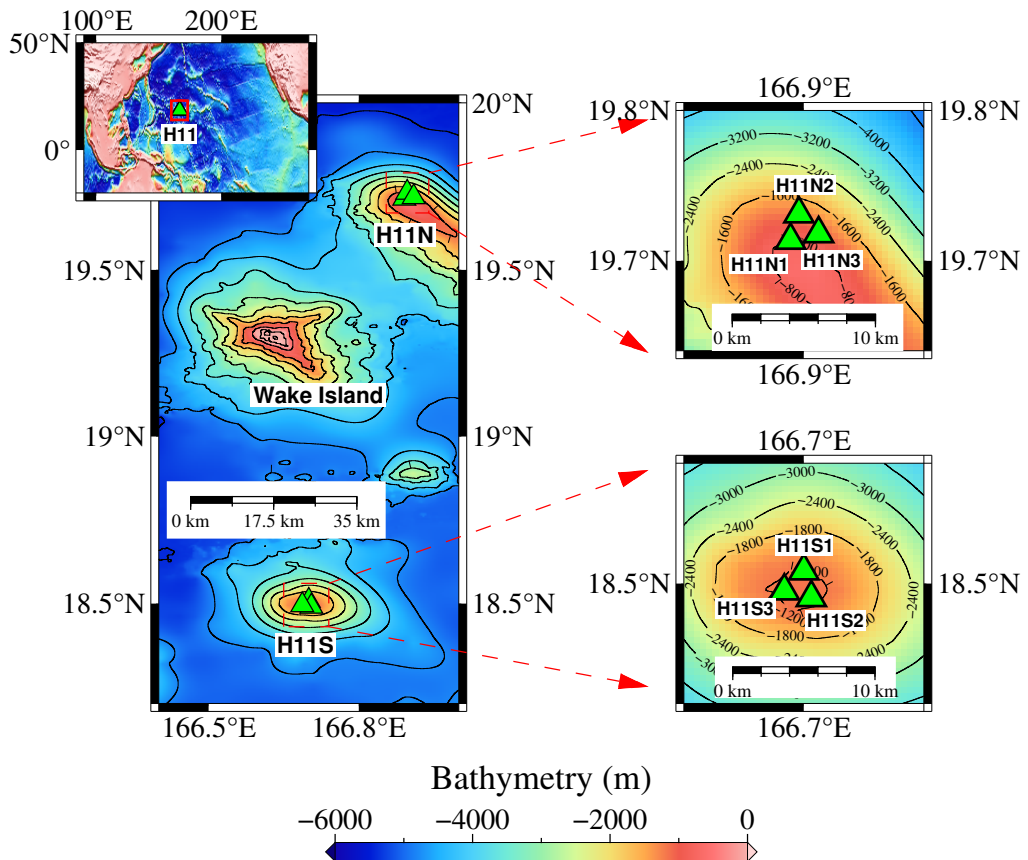
70

71 **Supplementary Note 3 | Verification of explosive submarine volcanic eruption**

72 There is no spatial or temporal overlap between the detected explosive submarine volcanic
73 eruptions and the reported earthquakes in the catalogs from the U.S. Geological Survey
74 (USGS) and the International Seismological Center (ISC) in the four regions of the Fukutoku-
75 Okanoba, Kaitoku, Ahyi and South Sarigon seamounts. Many detected explosive submarine
76 volcanic eruptions in those four regions can be independently confirmed by the observational
77 eruption evidence of discolored surface ocean water, bathymetry changes, tsunamis, lava
78 flows, pumice rafts and ash-steam plumes. We show an example for the detected Fukutoku-
79 Okanoba submarine volcanoes (Supplementary Fig. 7). Two visible ash-steam plume eruptions
80 and 67 discolorations of water on the sea surface were documented and time-stamped in the
81 Fukutoku-Okanoba submarine volcano region, by vision aerial and satellite observations and
82 pumice rafts conducted by the Japan Meteorological Agency (JMA) during 2010-2022¹¹⁻¹⁴.
83 Among the 471 explosive submarine volcanic eruptions detected in Fukutoku-Okanoba
84 (Supplementary Fig. 8a), 300 events occurred within a week from the two observed plumes on
85 03 February, 2010 and August 15, 2021 and 45 observed events of discolored surface sea water

86 (Supplementary Fig. 8). The other 171 detected events occurred in the time windows of no
87 collection of visual evidence (Supplementary Fig. 8). There are 22 observed events of
88 discoloration of water with no associated explosive submarine volcanic eruptions detected. In
89 those events, the discoloration of water occurred in small areas, likely caused by small
90 eruptions that escape the detection by the hydroacoustic data. Similarly, more than 88% of the
91 detected explosive submarine volcanic eruptions around Kaitoku, Ahyi and South Sarigon
92 seamounts can also be verified by the observed discoloring events in both the occurring time
93 and geographical location (Supplementary Figs. 9-11).

94

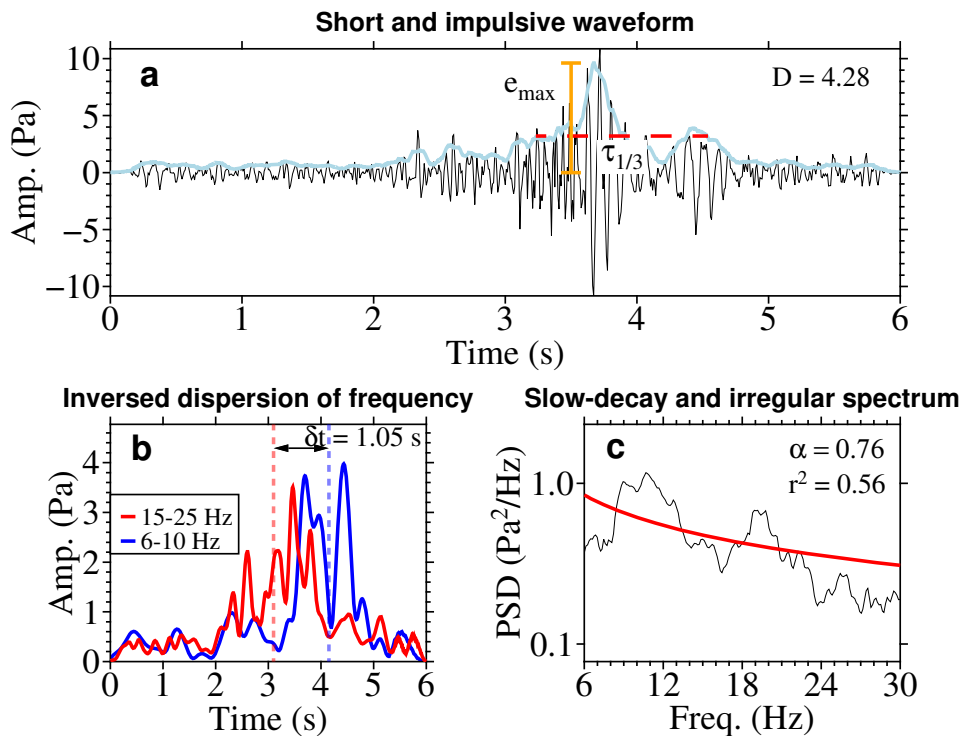


95

96 **Supplementary Fig. 1 | H11 hydrophone array used to study explosive submarine**
 97 **volcanoes.** Northern and southern subarrays (green triangles) are labeled as H11N and H11S
 98 respectively. Regions of red dashed box are enlarged and shown in the right panels with
 99 individual hydrophone stations labeled. Left-top inset shows the region (red box) in a broader
 100 region of the Pacific Ocean. Background color and black contours show bathymetry¹⁵.

101

102

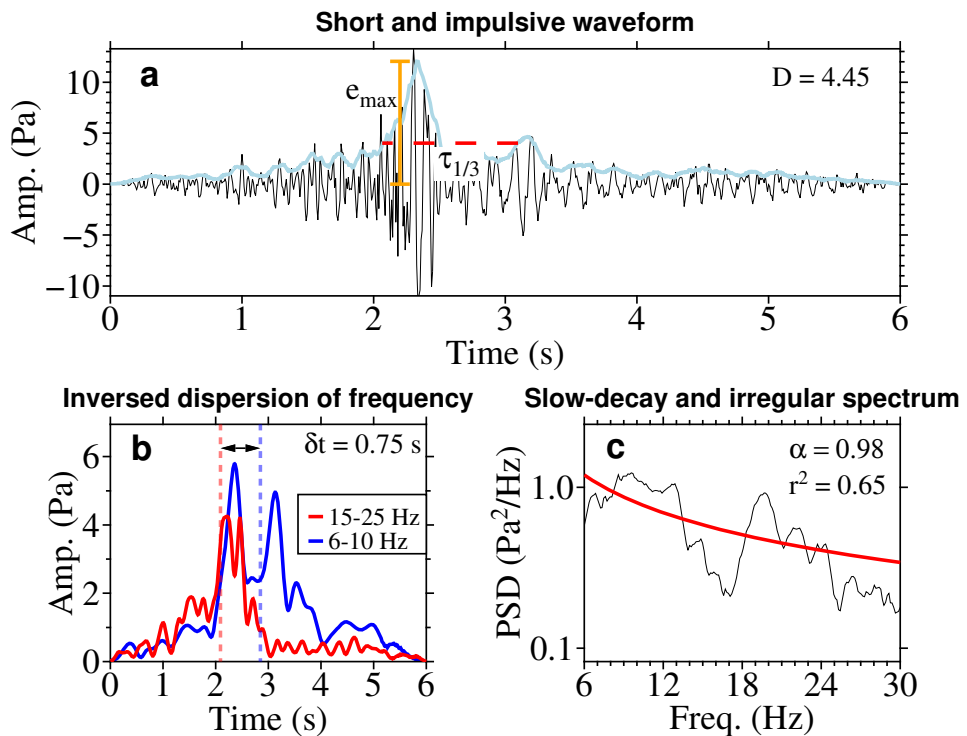


103

104 **Supplementary Fig. 2 | Same as Extended Data Fig. 2, except for hydrophone station**

105 **H11S2.**

106

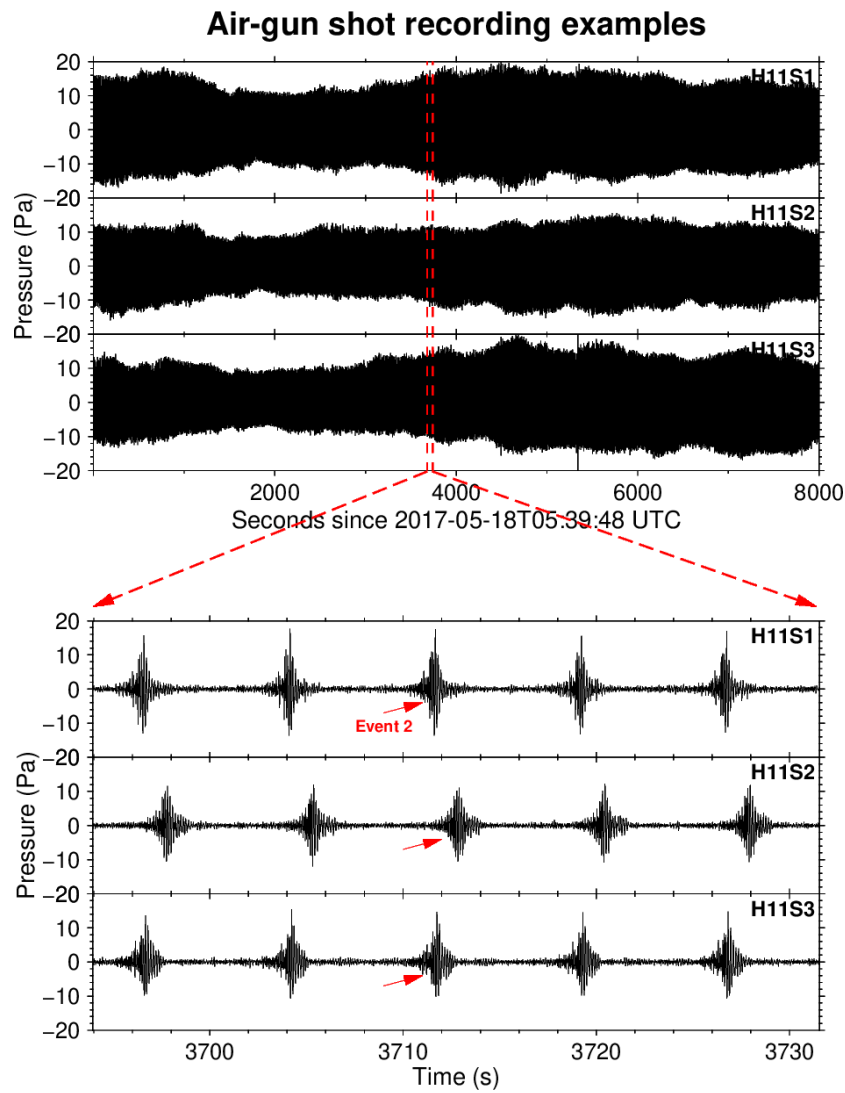


107

108 **Supplementary Fig. 3 | Same as Extended Data Fig. 2, except for hydrophone station**

109 **H11S3.**

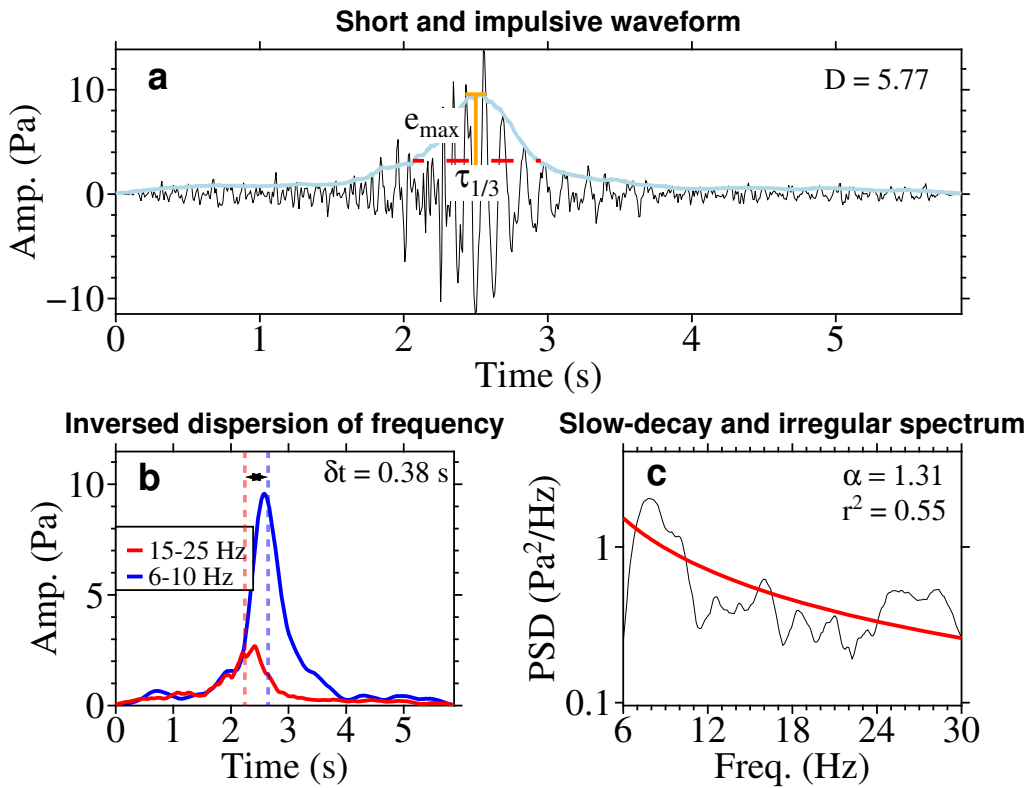
110



111

112 **Supplementary Fig. 4 | Waveform characteristics of air-gun shot signals.** (Top) 8000-s
 113 pressure recordings of air-gun shot signals at hydrophones H11S1, H11S2 and H11S3.
 114 (Bottom) Enlarged pressure recordings in the time window between the red dashed lines in the
 115 top panel. Red arrows in the bottom panel indicate an air-gun shot signal that is used to show
 116 its possession of similar seismic discriminants for the detection of an explosive submarine
 117 volcanic eruption in Supplementary Fig. 5.

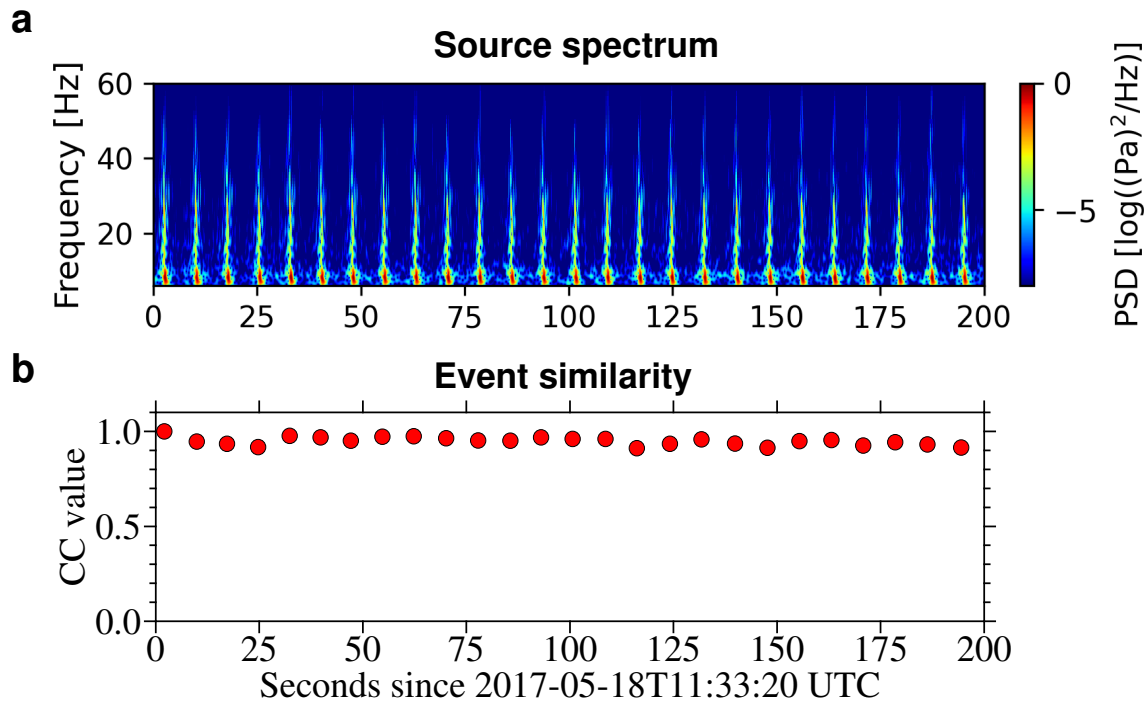
118



119

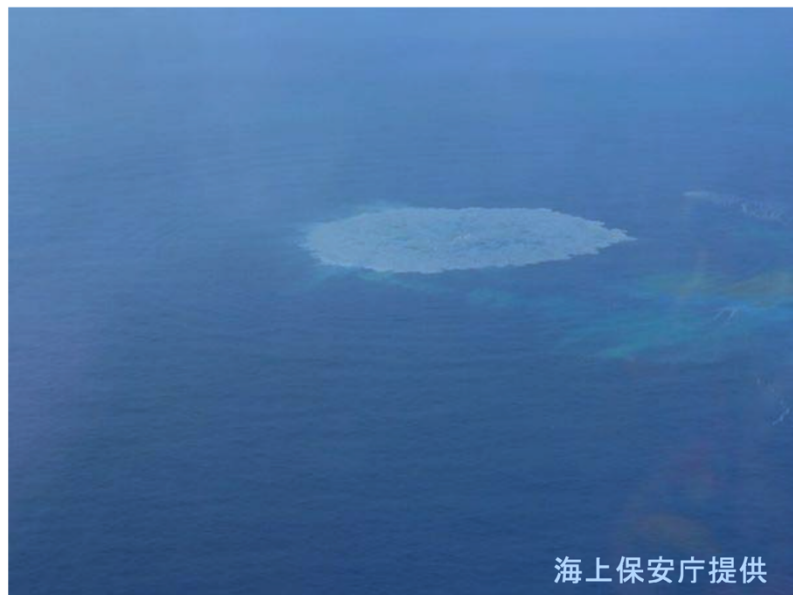
120 **Supplementary Fig. 5** | Same as Extended Data Fig. 2, except for an example air-gun shot
 121 indicated in Supplementary Fig. 4. Note the similarities of seismic discriminants between
 122 Supplementary Fig. 5 and Extended Data Fig. 2.

123



124 **Supplementary Fig. 6 | Source characteristics of air-gun shot signals. (a)** Source spectrum
 125 and **(b)** waveform similarity of example air-gun shot signals taken from 11:33:20 to 11:36:40
 126 UTC, on May 18, 2017. Red dots in **b** represent the cross-correlation values for each signal
 127 with the first signal in the time window. Note the similarities of source spectrum and
 128 waveforms between air-gun shots.
 129

130

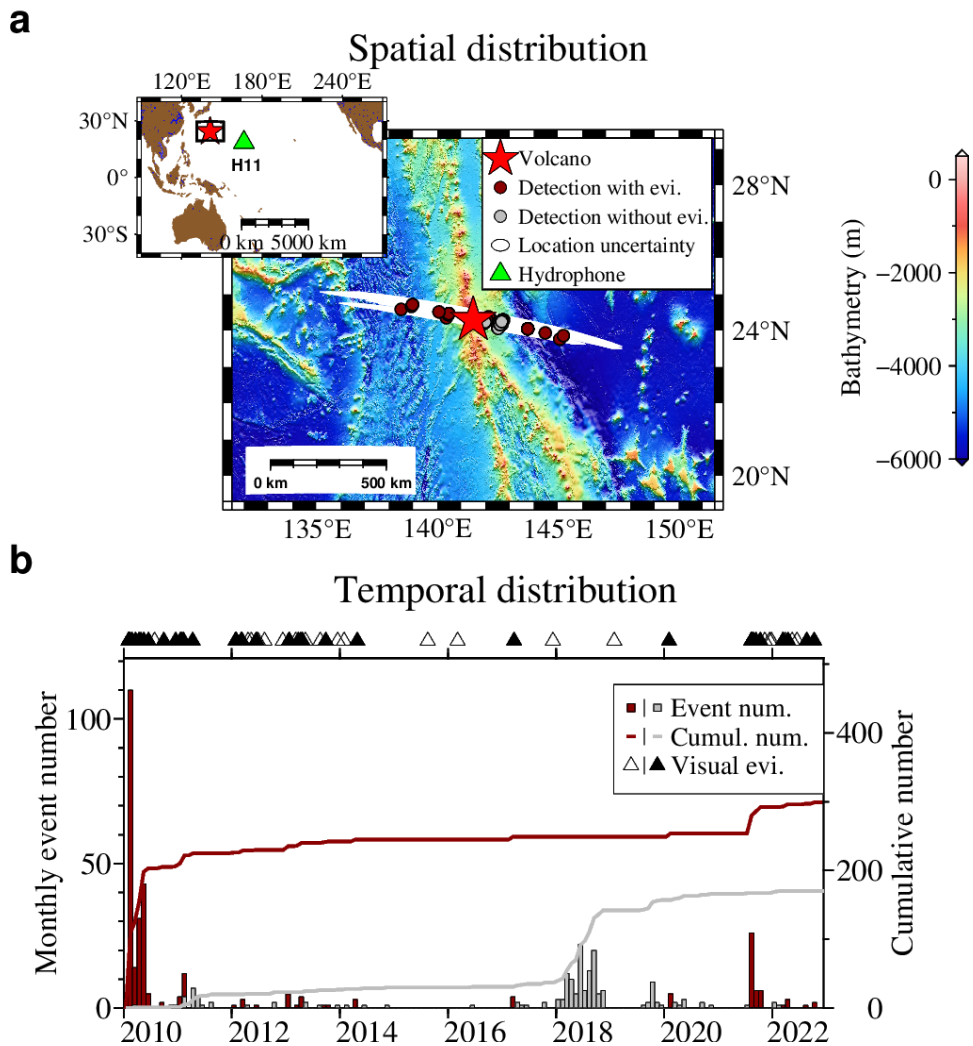


131

132 **Supplementary Fig. 7 | Discolored water spreading in a lotus pattern at 04:51 UTC on**
133 **February 4, 2010 observed by a local flyover photo near the sea surface of the Fukutoku-**
134 **Okanoba.** The source is issued by the Japan Meteorological Agency (JMA).

135

Verification of explosive submarine volcanic eruptions in Fukutoku-Okanoba

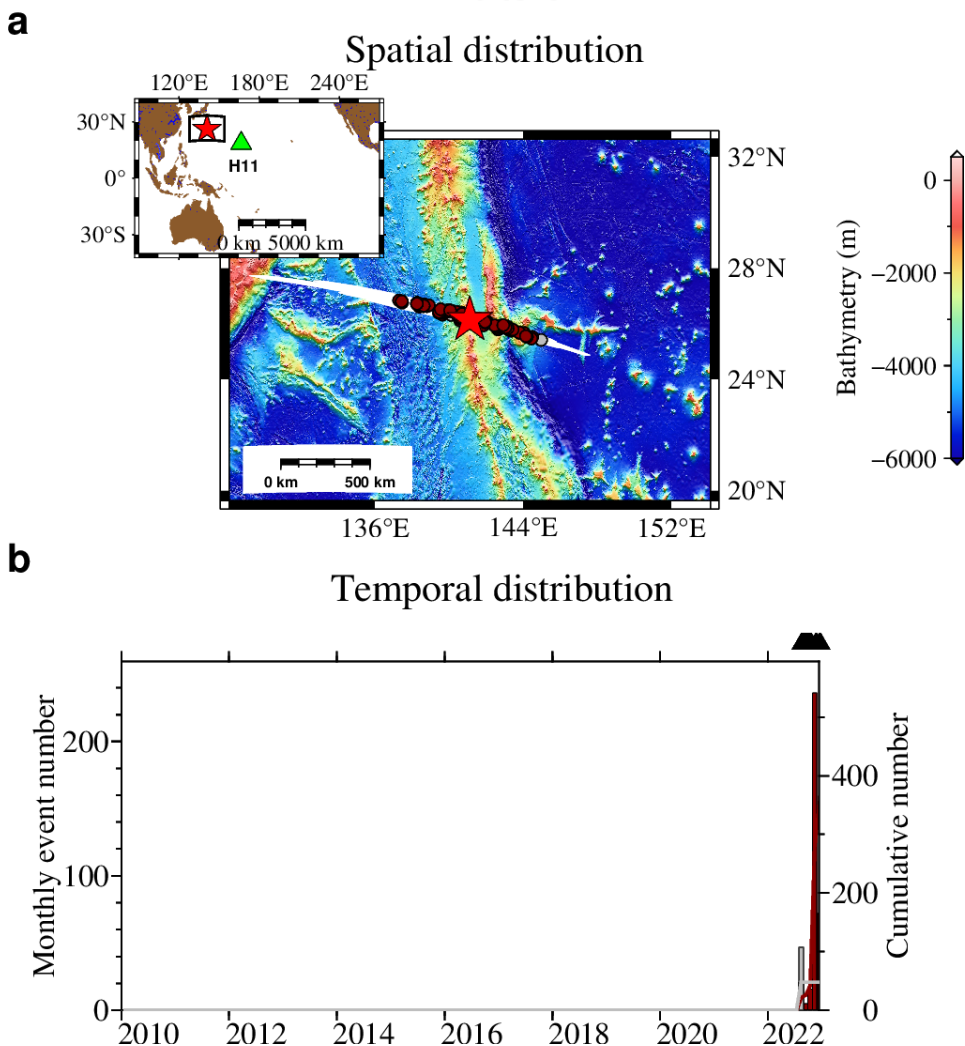


136 **Supplementary Fig. 8 | Detection and verification of explosive submarine volcanic**
137 **eruptions of Fukutoku-Okanoba in the northwest Pacific Ocean. a,** Locations of the
138 detected explosive submarine volcanic eruptions around Fukutoku-Okanoba (red star), with
139 those of red dots verified by the observed ocean surface coloring and those of gray dots without
140 verifiable ocean surface observation. White ellipses represent errors of the determined
141 locations of the events. The background color marks bathymetry. The left-top inset shows the
142 region (black box) in a broader region with the H11 hydrophone array (green triangle). **b,**
143 Numbers of the detected explosive submarine volcanic eruptions from 2010 to 2022, with the
144 monthly numbers represented by bars (the left vertical axis for scale), and the cumulative
145 numbers represented by curves (the right vertical axis for scale). The bars and curves are color-

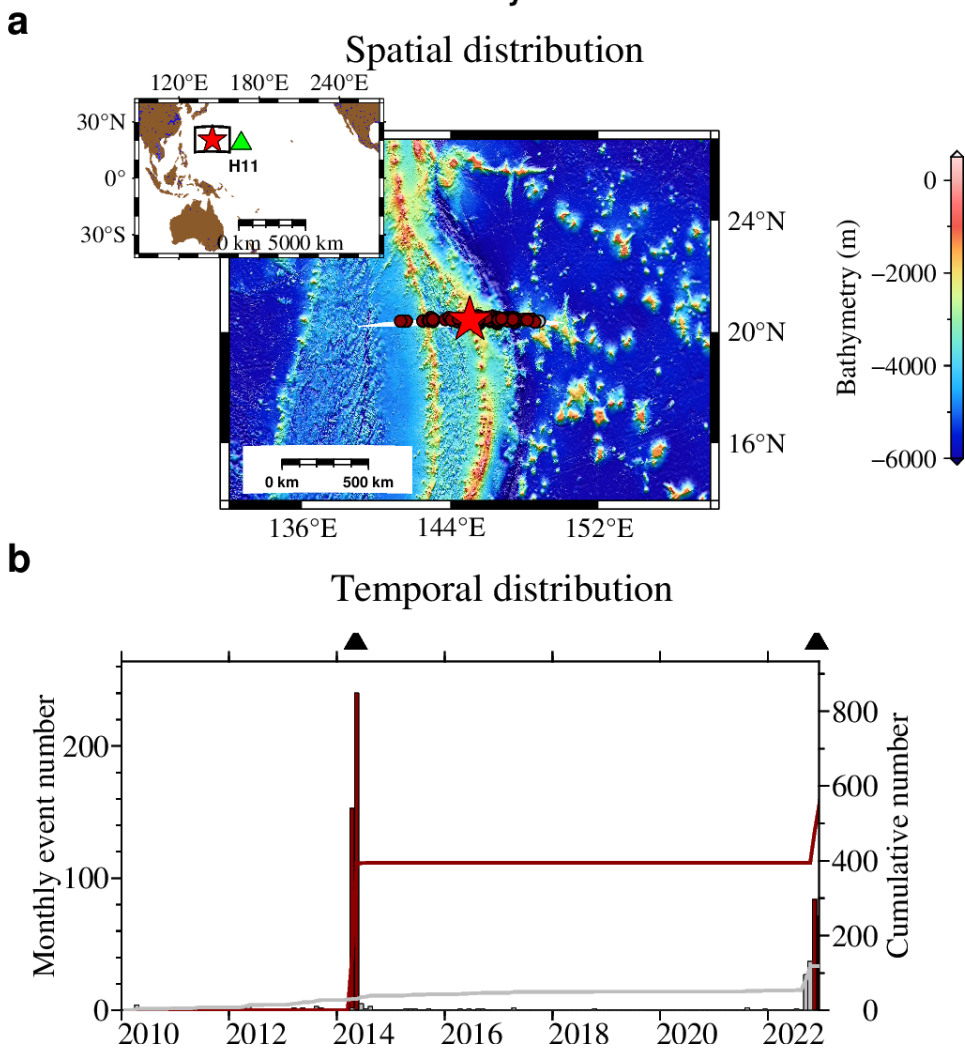
147 coded with the dots in **a**. Symbols above the panel indicate the observed visual eruption events,
148 with filled and blank triangles representing visual eruption events with and without associated
149 detections of submarine volcanic eruption within a week of the event.

150

**Verification of explosive submarine volcanic eruptions
in Kaitoku**

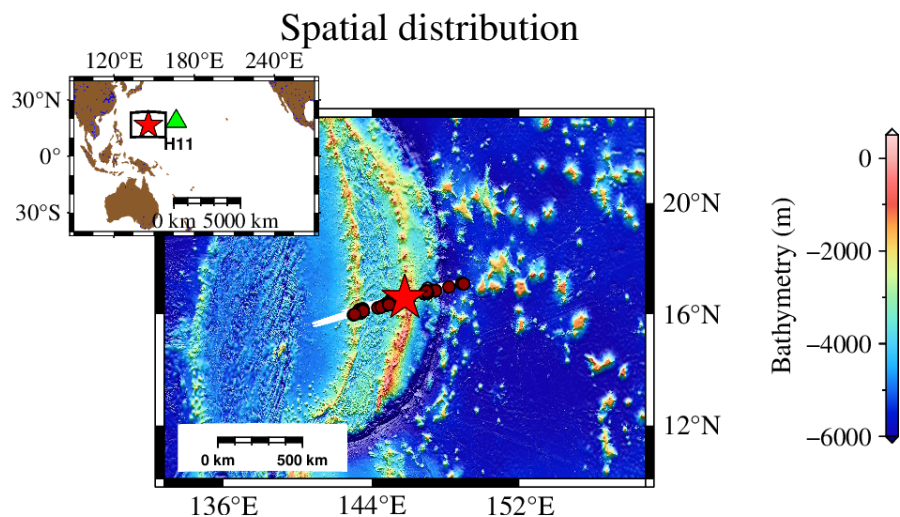


**Verification of explosive submarine volcanic eruptions
in Ahyi**

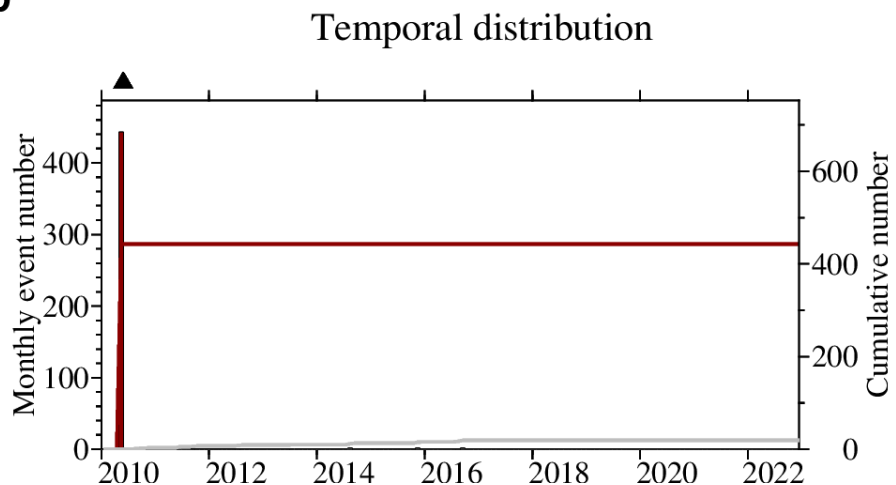


**Verification of explosive submarine volcanic eruptions
in South Sarigon**

a



b



163 **Supplementary References**

164 1 Hanson, J. *et al.* Operational processing of hydroacoustics at the Prototype International
165 Data Center. *pure and applied geophysics* **158**, 425-456 (2001).
166 2 Green, D. N. *et al.* Hydroacoustic, infrasonic and seismic monitoring of the submarine
167 eruptive activity and sub-aerial plume generation at South Sarigan, May 2010. *Journal*
168 *of Volcanology and Geothermal Research* **257**, 31-43 (2013).
169 3 Bohnenstiehl, D. R., Dziak, R. P., Matsumoto, H. & Conder, J. A. Acoustic response
170 of submarine volcanoes in the Tofua Arc and northern Lau Basin to two great
171 earthquakes. *Geophysical Journal International* **196**, 1657-1675 (2014).
172 4 Tepp, G. *et al.* Hydroacoustic, seismic, and bathymetric observations of the 2014
173 submarine eruption at Ahyi seamount, Mariana Arc. *Geochemistry, Geophysics,*
174 *Geosystems* **20**, 3608-3627 (2019).
175 5 Talandier, J., Hyvernaud, O., Hébert, H., Maury, R. C. & Allgeyer, S. Seismic and
176 hydroacoustic effects of the May 29, 2010 submarine South Sarigan volcanic explosion:
177 Energy release and interpretation. *Journal of Volcanology and Geothermal Research*
178 **394**, 106819 (2020).
179 6 Bromirski, P. D., Duennebier, F. K. & Stephen, R. A. Mid - ocean microseisms.
180 *Geochemistry, Geophysics, Geosystems* **6** (2005).
181 7 Reeves, R. R. The origins and character of 'aboriginal subsistence' whaling: a global
182 review. *Mammal Review* **32**, 71-106 (2002).
183 8 Širović, A., Wiggins, S. M. & Oleson, E. M. Ocean noise in the tropical and subtropical
184 Pacific Ocean. *The Journal of the Acoustical Society of America* **134**, 2681-2689
185 (2013).
186 9 ZHAO, M. H. *et al.* Large Volume Air - Gun Sources and Its Seismic Waveform
187 Characters. *Chinese Journal of Geophysics* **51**, 400-408 (2008).
188 10 Dragoset, B. Introduction to air guns and air-gun arrays. *The leading edge* **19**, 892-897
189 (2000).
190 11 Yoshida, K. *et al.* Variety of the drift pumice clasts from the 2021 Fukutoku - Oka -
191 no - Ba eruption, Japan. *Island Arc* **31**, e12441 (2022).
192 12 Matsumoto, H. *et al.* Interpretation of detections of volcanic activity at Ioto Island
193 obtained from in situ seismometers and remote hydrophones of the International
194 Monitoring System. *Scientific Reports* **9**, 19519 (2019).
195 13 Global Volcanism Program. Report on Fukutoku-Oka-no-Ba (Japan) (Bennis, K.L.,
196 and Venzke, E., eds.). *Bulletin of the Global Volcanism Network* **46**, Smithsonian
197 Institution, doi:<https://doi.org/10.5479/si.GVP.BGVN202111-284130>. (2021).
198 14 Global Volcanism Program. Report on Fukutoku-Oka-no-Ba (Japan) (Sennert, S, ed.).
199 *Weekly Volcanic Activity Report 29 December-4 January 2022*, Smithsonian
200 Institution and US Geological Survey (2021).
201 15 Tozer, B. *et al.* Global bathymetry and topography at 15 arc sec: SRTM15+. *Earth and*
202 *Space Science* **6**, 1847-1864 (2019).
203
204